AIAA AVIATION Forum
June 25-29, 2018, Atlanta, Georgia
2018 Applied Aerodynamics Conference

10.2514/6.2018-3001

A Multi-objective Multi-disciplinary Optimization Approach for NATO AVT 251 UCAV – MULDICON

Ali Karakoç[1]
Defense Industries Research and Development Institute, Ankara, 06261, Turkey

Halil Kaya[2]
Turkish Aerospace Industries Inc., Ankara, 06980, Turkey

The present study aims to develop an aerodynamics and RCS signature optimization approach for NATO AVT – 251 Task Group's UCAV configuration MULDICON. The approach incorporates design of experiment, the concept of surrogate models and multi-objective genetic algorithm. In the present study, as an application of the approach, MULDICON configuration was optimized to increase CL max (usable), which is defined as CL value where large local gradient change of static stability appears, by keeping survivability the same as the baseline geometry in terms of the defined RCS objective value.

Nomenclature

CFD	Computational Fluid Dynamics
C_L	Lift force coefficient
dB	Decibel
DOE	Design of Experiment
E	Field intensity
ft	Feet
G	Gain
MDO	Multi-Disciplinary Optimization
MOGA	Multi-Objective genetic Algorithm
P	Power
r	Receiver
RANS	Reynolds Averaged Navier-Stokes
RCS	Radar Cross Section
SACCON	Stability and Control Configuration
SU2	Stanford University Unstructured
t	Transmitter
UCAV	Unmanned Combat Aerial Vehicle
σ	Radar Cross Section Value
λ	Wave length

I. Introduction

The NATO STO AVT-251 Multi-disciplinary design and performance assessment of effective, agile NATO air vehicles Task Group [1] aims to redesign The STO/AVT aerial configuration SACCON based on the given requirements and to demonstrate the performance of the designed configuration based on these requirements. One of the design requirements indicates $C_{L\,max}$ at take-off conditions.

At low speed the aerodynamic characteristic of UCAV configuration is highly affected by a vortical flow field. Moreover, the vortical flow topology has a strong sensitivity to changes in angle of attack and this sensitivity results

[1] System Engineering and Stealth Specialist, ali.karakoc@tubitak.gov.tr
[2] Aerodynamics Specialist, UAV Group, hkaya@tai.com.tr

a highly non-linear behavior in pitching moment. If the local gradient change of static stability is large, it could represent a major problem for stabilization. Generally, an abrupt change in static stability occurs before $C_{L\ max}$ is reached. Hence, a new term "$C_{L\ max\ (usable)}$" is defined, that is C_L value where large local gradient change of static stability appears.
In the present study, due to absence of an explicit value for acceptable gradient change value in pitching moment, an assumption has been made and the maximum acceptable change of $C_{M\alpha}$ with respect to angle of attack was specified as 0.002. In the Figure 1, the acceptable limit is depicted by the redline.

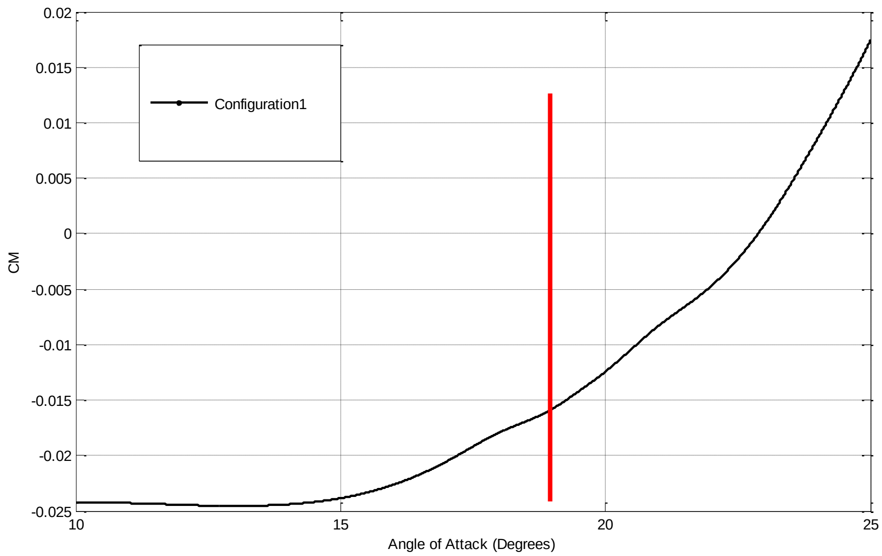

Figure 1 The Maximum acceptable change of CM_α

For stealth aircrafts like MULDICON, detection range is also one of the most important performance metrics. Hence, it is also necessary to care survivability in an acceptable level, whereas improving $C_{L\ max\ (usable)}$. Therefore, as another design requirement, it is intended that RCS signature values of the optimized geometry are lower than the RCS signature value of the base geometry. This target objective is also employed into the optimization algorithm.

II. Numerical Method

A. Design Variables

According to the study [2], leading edge radii and twist angles of the profiles have significant influence on the vortex flow topology development. So, leading edge radii and twist angles of the airfoil B and airfoil C, which are illustrated in the Figure 2, are employed as design variables. The base geometry was MULDICON official design 2. The design space is also given in Figure 2.

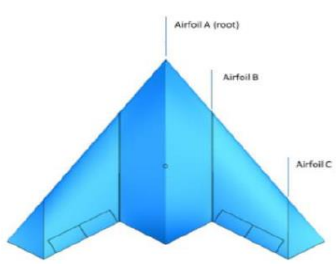

	*leading edge radius ratio		Incidence angle	
Airfoil	mininum	maximum	mininum	maximum
B	1	2	-1^0	-3^0
C	1	2	-4	-6

*Leading edge radius ratio: leading edge radius of generated profile/initial leading edge radius

Figure 2 The design variables and the design space

The geometries that correspond to the selected design points and the surface meshes of the geometries required for RCS analyses were generated employing OpenVSP scripting.

B. Flow Solver

A high-fidelity aerodynamic analysis tool like a RANS flow solver is necessary to be able to predict the phenomenon such as flow separation, vortex breakdown etc.. In the present study, the open source Stanford University Unstructured (SU2) software package [3] is utilized for prediction of $C_{L\ max\ (usable)}$. The SU2 suite is developed for the analysis of partial differential equations (PDE) and PDE-constrained optimization problems on unstructured grids. Although the suite is general, it mainly focused on RANS solver capable of simulating compressible, turbulent flows. Moreover, the verification and validation of the software within the context of compressible, turbulent flows described by RANS equations is presented in the reference [4].

In the present study, steady-state simulations were performed. Inviscid fluxes were computed using Roe's flux-difference splitting [5]. For second order accuracy, the gradients of flow variables were computed employing weighted least- squares technique. For time integration, Euler implicit scheme was applied. As a turbulence model, one equation Spalart-Allmaras turbulence model was employed. The turbulence working variable was convected using a first-order, scalar upwind method. The viscous fluxes were calculated using the corrected average gradient method.

C. Computational Domain

The computational grids (Figure 3) were generated Pointwise's meshing software. Moreover, mesh generation process was automated using Pointwise's Glyph scripting language. The computational grids were generated on half geometry. The surfaces of the wings were discretized using ≈200 K triangular elements. The height of the first viscous layer was 3e-6 m that ensures $y^+<1$ over the airfoil surface. Moreover, there were 35 viscous layers generated with 1.25 growth rate. The computational grids composed of ≈22 M hybrid volume elements (prisms, tetrahedral and pyramids).

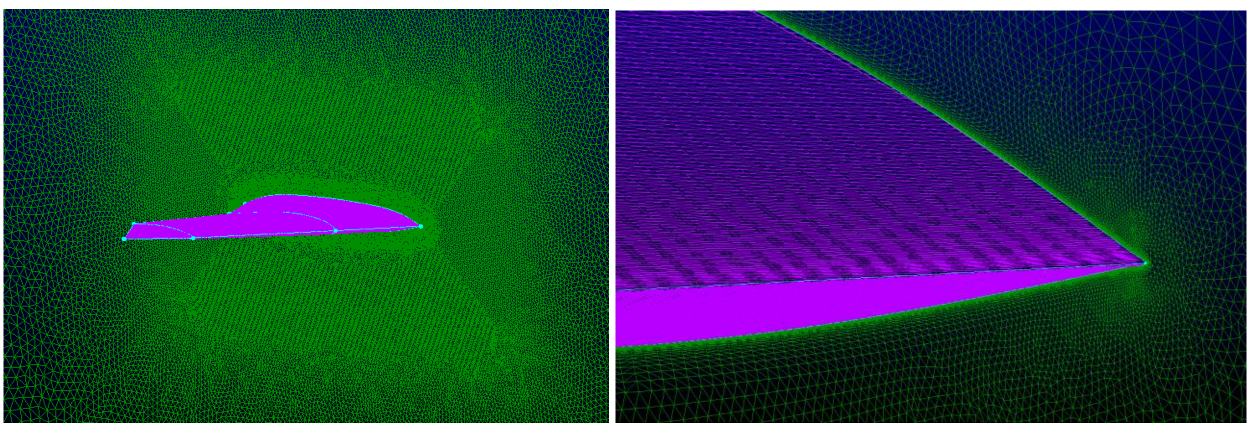

Figure 3 Computational Grid

D. Radar Cross Section Solver

Radar cross section (RCS) is a measure scattering received at a receiver from an object. RCS is defined in IEEE [6] as 'For a given scattering object, upon which a plane wave is incident, that portion of the scattering cross section corresponding to a specified polarization component of the scattered wave'. The RCS can be defined in terms of incident and scattered field intensities as

$$\sigma = \lim_{R\to\infty} 4\pi R^2 \frac{|E_s|^2}{|E_i|^2} \tag{1}$$

Where, E_s and E_i are the scattered and incident field intensities, respectively. RCS analysis and control are already studied and explained in several books in literature [7], [8], [9]. In this paper, only basic explanations are given to understand the significance of the RCS.

The radar equation in a simple form can be expressed as

$$P_r = \left(\frac{P_t G_t}{4\pi R^2}\right)\left(\frac{\sigma}{4\pi R^2}\right)\left(\frac{G_r \lambda^2}{4\pi}\right) \tag{2}$$

where, P_r is the power received by the radar, P_t is the output power of the transmitter, G_t and G_r are the gains of transmitter and receiver antenna, respectively, σ denotes the radar cross section of the target, λ represents the wavelength of the radar's frequency, and R is the range between the radar and target. The first term in the parenthesis at the right side of the equation is the power density at the target (watts/m^2). The product of the first and second terms in the parenthesis represents the power density at the radar receiver. Finally, the third term is the power captured by the receiving antenna. The RCS is called as monostatic if the transmitter and the receiver are collocated.

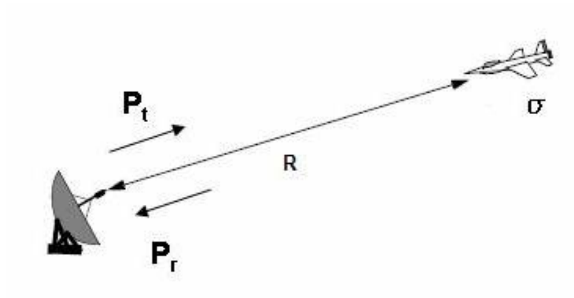

Figure 4 Generic Radar-Target Configuration (Monostatic)

For the monostatic radar configuration as shown in Figure 4, where

$$G = G_t = G_r \tag{3}$$

Then, Eq. (2) can be rewritten as

$$P_r = \frac{P_t G^2 \sigma \lambda^2}{(4\pi)^3 R^4} \tag{4}$$

The range of radar is defined as the distance beyond which the target cannot be detected. Hence,

$$R_{radar} = \left(\frac{P_t G^2 \sigma \lambda^2}{(4\pi)^3 S_{min}}\right)^{1/4} \tag{5}$$

where S_{min} is the threshold value for the signal which can be detected by the receiver. Eq. (5) shows that detection range of radar is proportional to $\lambda^{1/4}$. If the RCS of the target is reduced by a factor of 16, free detection range decreases 50%. Table 1 illustrates the effect of RCS reduction on the target detection range.

Table 1 Effect of RCS Reduction on the Detection Range [10]

RCS Reduction, %	RCS Reduction, dB	Detection Range
0	0	100 (arbitrary)
90	10	56
99	20	32
99.9	30	18
99.99	40	10

Figure 5 illustrates the effect of RCS on the detection range for a target flying at an altitude of 10000 ft [11]. As the transmitted power of the radar increases, detection range gets larger. Furthermore, reduction in RCS reduces detection range, beyond which no threat is encountered, significantly.

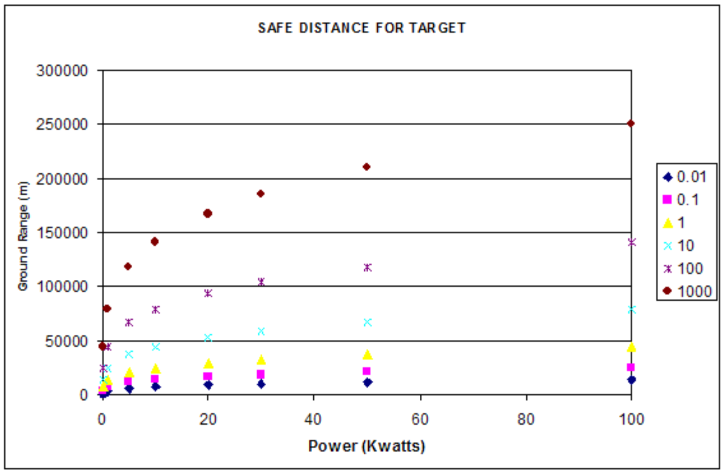

Figure 5 Effect of RCS on the Detection Range

The RCS is usually expressed in decibels relative to a square meter (dBsm):

$$\sigma[dBsm] = 10\log(\sigma)[m^2] \tag{6}$$

The RCS of a target is dependent on several parameters listed below:

- Geometry of the target,
- Material (s) of the target,
- Frequency of incident,
- Polarization of the radar,
- Positions of antennas relative to the target.

The most common RCS prediction methods are the Finite Difference Method, the Method of Moments, Microwave Optics (the Geometrical Optics method and the Geometrical Theory of Diffractions method) and the Physical Optics. In the present study, the Physical Optics method was utilized for the prediction of RCS. The Physical Optics method approximates the surface currents induced on the surface by setting them to be simply proportional to incident magnetic field intensity on the illuminated side of the body using geometrical optics. On the shadowed portion, the current is set to zero. The currents are used to compute the radiation integrals. The method provides good results for electrically large targets (at least 10 wavelengths in size). The method does not include surface waves, multiple reflections and edge diffractions [8]. To improve the accuracy of the solver a basic Geometrical Optics code was also incorporated into the main code which is utilized for the prediction of RCS by the way of Shooting and Bouncing Rays method to calculate the multiple reflections up to 3. Using the principles of the optics, the rays bounce from the walls and finally leave the cavity by the gaps. Vectored integration of the bouncing rays is calculated on the backscattered field from the exit rays. For high frequency microwaves the method is simple and easy to use by short time calculation afford. Total accuracy of the method is lower than Finite Difference Method and the Method of Moments but enough to estimate pick RCS values on the geometry though conceptual design phase.
Model of the target is established by means of Solid Modeling Program and exported to RCS prediction software in STL (Stereo-Lithographic) format. Furthermore, illumination condition (illuminated or shadowed) and resistivity information for each facet is supplied. RCS prediction software processes the model and the facet information to compute RCS for required frequency and orientation values. Coordinate system utilized is shown in Figure 6.

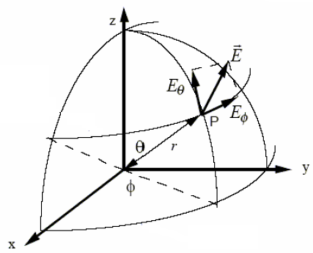

Figure 6 Coordinate System

E. Optimization

To be able to achieve the defined objectives, a surrogate based optimization methodology was employed. The methodology can be utilized to get global optima in the given design space. The main idea behind the surrogate modeling is to build a simplified mathematical approximation for an objective function with respect to design variables. Since the approximated model of objective function with respect to design variables mimics the original high fidelity simulation tool within the range of design space, one may utilize surrogate model to perform an optimization study or to explore design space. That's why, the methodology is of particular interest for engineering design when high-fidelity analyses employed.

To construct a surrogate model, it is necessary to obtain sample data by running the high-fidelity simulation. The determination of sample locations is also an issue of importance. The sample locations should be selected such that the sampled data give maximum information with the limited number of sample points. Therefore, to be able to get maximum information from limited number of sample points, a design of experiment method was employed. The selected DOE method is the Latin hypercube sampling. In the present study to build a surrogate model for the objective functions with respect to 4 design variables, 18 sample points were selected. Then, at the selected sample points, aerodynamic and RCS analyses were performed. Aerodynamic analyses were performed at one degree of angle of attack intervals in the range from -10^0 to 25^0. The calculated pitching moment coefficients of the selected design points are given in the Figure 7 and calculated RCS objective values are given in the Figure 8. Moreover, the calculated $C_{L\ max\ (usable)}$ value of the base geometry is 0.921 and calculated RCS objective value is 13.25%.

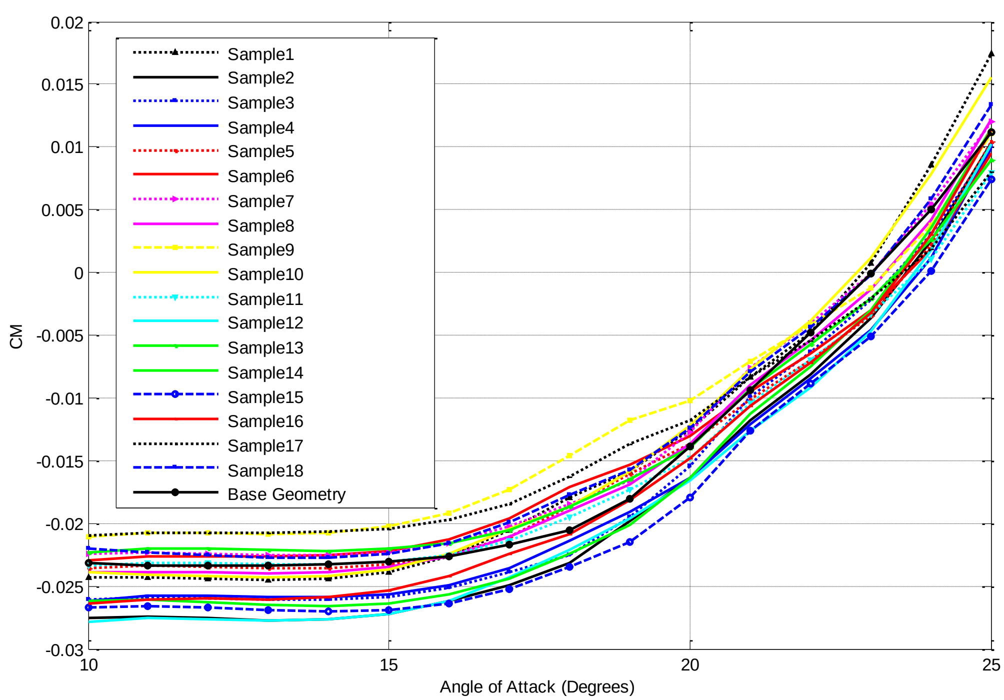

Figure 7 The calculated pitching moment coefficients of the selected sample points

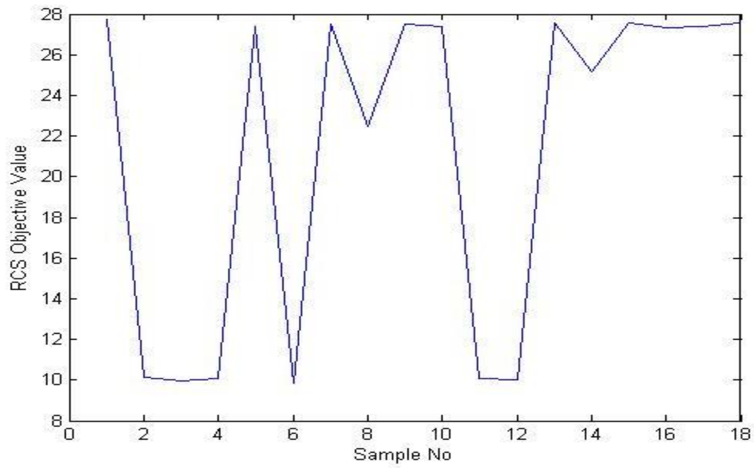

Figure 8 RCS Objective Value vs Sample Point

The mathematical model approximations for the calculated objective functions were performed using Kriging approximation technique. The qualities of the approximated models are considered by leave-one-out cross-validation technique. The comparison of the predicted value by leave-one-out cross-validation and the calculated value at sample points are illustrated in the Figure 9. The mean absolute error of the aerodynamic objective function was 2E-16 and the mean absolute error of the radar cross section objective function was 7E-14.

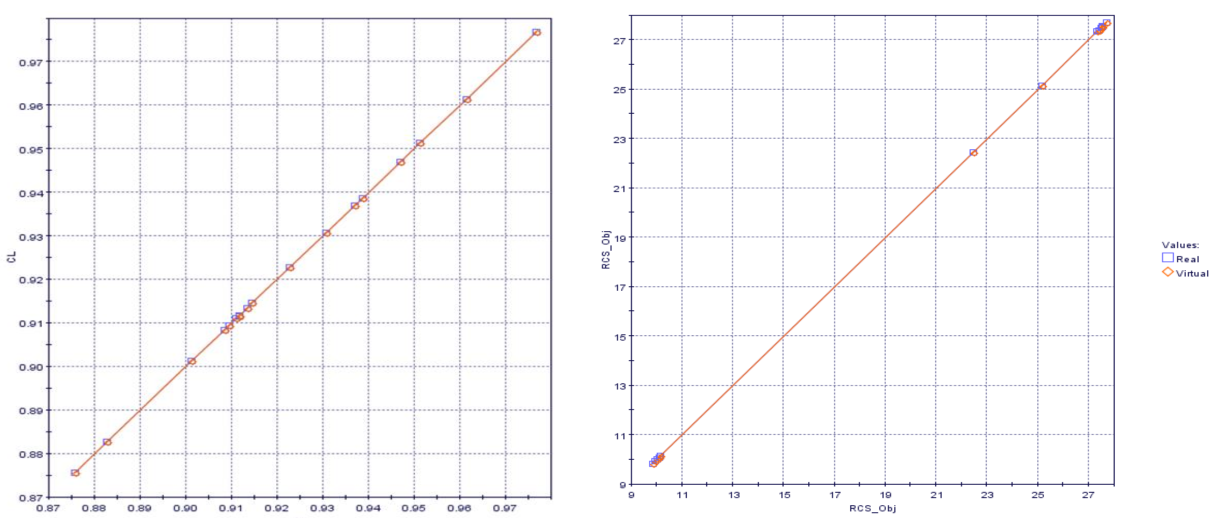

Figure 9 Leave-one-out cross validation for the objectives

In the present study, the optimization problem is to increase $C_{L\ max\ (usable)}$, which is defined as C_L value where large local gradient change of static stability appears, at take-off condition by keeping the defined RCS objective value constant. The defined RCS objective value is the percentage of the number of angles, at which RCS signature values are greater than 1 m^2, to the number of angles at which RCAS analyses were conducted The targeted value of RCS objective is the RCS objective value of the baseline design which is 13.25%. The RCS analysis result of the baseline geometry is given in the Figure 10. The angles, at which RCS signature values are greater than $1m^2$, colored by red.

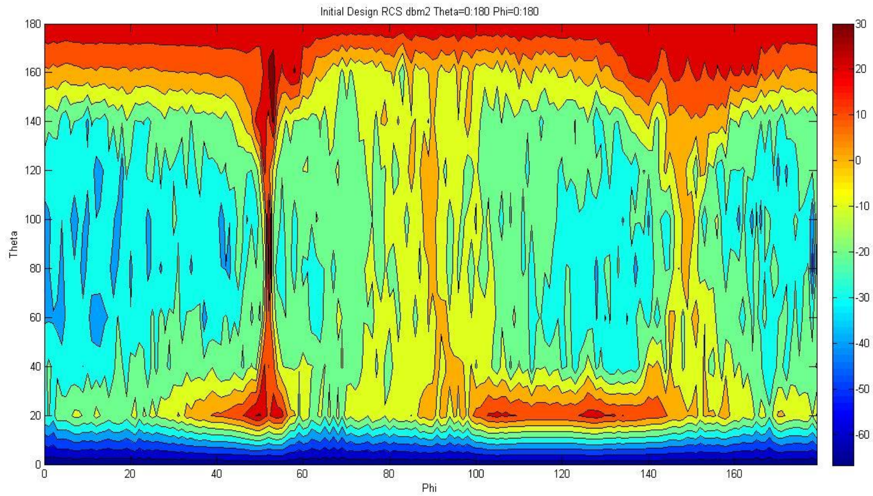

Figure 10 RCS analysis result of the baseline geometry

The defined MDO problem was solved by using the MOGA-II (Multi-Objective Genetic Algorithm) to get Pareto Frontier. MOGA-II is one of the evolutionary algorithms which involve elitism sorting procedure in every generation; by using this algorithm one can prevent the loss of good solutions once they are found [12]. Multi Objective Genetic Algorithm (MOGA-II) with a simple constraint handling method was applied to find Pareto optimal solutions of this bi-objective optimization problem.

III. Results and Discussion

To be able to achieve the defined objectives, a multi-objective, meta-model-based design optimization was employed and % 13.27 stealth qualities and 1.01 $C_{L\ max\ (usable)}$ achieved. The improvement in $C_{L\ max\ (usable)}$ is shown in the Figure 12. Calculated RCS and RCS objective values without meta-models are shown in Figure 11, red colored lines are initial design values. Meta-model results included the error values and pareto frontiers with selected optimum design shown in Figure 12.

The study shows that it is possible to get aerodynamic improvement whereas keeping stealth characteristics of the aircrafts in acceptable value. But to get a final optimum design in conceptual phase it is necessary not only to include Aero-RCS characteristics into the MDO study but also structural constraints, aeroelasticity concerns, flight mechanical analyses and weighting calculations should be added. This would be very time consuming and difficult to handle but the study also shows that by using stochastic methods like meta-models is a good way to predict pretty good values. Also, to include inlet design into MDO study would be very helpful to predict total performance values in RCS and aerodynamic parameters.

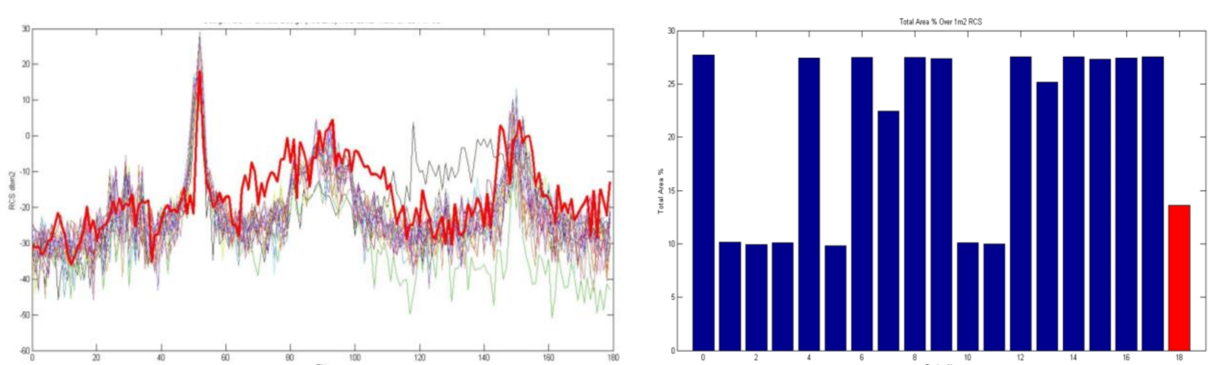

Figure 11 Calculated RCS and RCS Objective Results without Metamodels

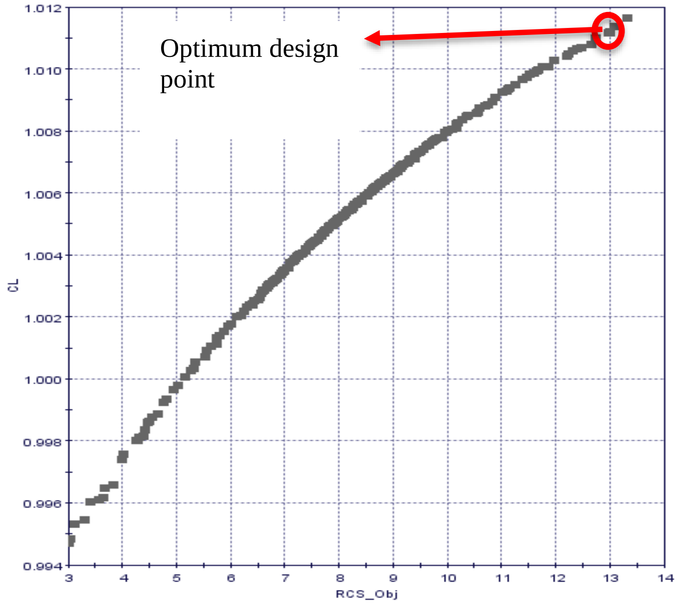

Initial and Targeted Design Value=13.25
Estimated Optimum RCS Obj =13.25
Analysed Optimum RCS Obj =13.27
Error=0.15 %

Initial Design Value $C_{L\ max\ (usable)}$=0.921
Estimated Optimum $C_{L\ max\ (usable)}$ =1.011
Analysed Optimum $C_{L\ max\ (usable)}$ =0.998
Error=1.3 %

Figure 12 Pareto Frontiers and Selected Model Included Metamodels

References

[1] R.M. Cummings, C. Liersch, A. Schütte, "Multi-Disciplinary Design and Performance Assessment of Effective, Agile NATO Air Vehicles," AIAA Aviation and Aeronautics Forum and Exposition, Atlanta GA, June 2018.

[2] Andreas Schütte. "Numerical Investigations of Vortical Flow on Swept Wings with Round Leading Edges", Journal of Aircraft, Vol. 54, No. 2 (2017), pp. 572-601.

[3] Thomas D. Economon, Francisco Palacios, Sean R. Copeland, Trent W. Lukaczyk, and Juan J. Alonso. "SU2: An Open-Source Suite for Multiphysics Simulation and Design", AIAA Journal, Vol. 54, No. 3 (2016), pp. 828-846.

[4] Palacios, F., Economon, T.D., Aranake, A. C., Copeland, S. R., Lonkar, A. K., Lukaczyk, T. W., Manosalvas, D. E., Naik, K. R., Padron, A. S., Tracey, B., et al., "Stanford University Unstructured (SU2): Open-source analysis and design technology for turbulent flows, "AIAA paper, Vol. 243, 2014, pp. 13-17.

[5] Roe, P. L., "Approximate Riemann Solvers, Parameter Vectors, and Difference Schemes, "Journal of Computational Physics, Vol. 43, No.2, 1981, pp. 357-372.

[6] IEEE Standart Definitions of Trems for Antennas, IEEE Trans. on Antennas and Propagation, Vol. Ap-31, No. 6, Nov. 1983.

[7] Jenn, D. C., Radar and Laser Cross Section Engineering, AIAA Education Series, 1995.

[8] Knott, E., Shaeffer, J., and Tuley, M., Radar Cross Section, 2nd Ed., Artech House, 1993.

[9] Bhattacharyya, A. K., and Sengupta, D. L., Radar Cross Section Analysis and Control, Artech House, 1991.

[10] Nathan, R. H., and Mavris, D. N., "A Parametric Design Environment for Including Signatures Analysis in Conceptual Design, 2000 World Aviation Conference, San Diego, CA, Oct. 10-12, 2000.

[11] Fleeman E. L., Tactical Missile Design, AIAA Education Series, 2001.

[12] Poles S., "MOGA II An Improved Multi Objective Genetic Algorithm", Esteco Technical Report, Dec. 2006.

[13] Kuran, B., Karakoç, A., Budak, T., Survivability Using Surrogate Models for The Design Optimization of Tactical Missiles: Artificial Neural Networks For The External Configuration Design Including Survivability, AIAC, 2007